

Please cite the Published Version

Pratt, Jaylene S, Ross, Stephanie A, Wakeling, James M and Hodson-Tole, Emma F (2021) EMG Signals Can Reveal Information Sharing between Consecutive Pedal Cycles. *Medicine and Science in Sports and Exercise*, 53 (11). pp. 2436-2444. ISSN 0195-9131

DOI: <https://doi.org/10.1249/mss.0000000000002727>

Publisher: Lippincott, Williams & Wilkins

Version: Accepted Version

Downloaded from: <https://e-space.mmu.ac.uk/628453/>

Usage rights:  Creative Commons: Attribution-Noncommercial 4.0

Enquiries:

If you have questions about this document, contact openresearch@mmu.ac.uk. Please include the URL of the record in e-space. If you believe that your, or a third party's rights have been compromised through this document please see our Take Down policy (available from <https://www.mmu.ac.uk/library/using-the-library/policies-and-guidelines>)

1 **EMG signals can reveal information sharing between consecutive pedal cycles**

2 **Jaylene S. Pratt¹, Stephanie A. Ross¹, James M. Wakeling¹, Emma F. Hodson-Tole²**

3 ¹Department of Biomedical Physiology and Kinesiology, Simon Fraser University, Burnaby, BC,
4 Canada

5 ²Musculoskeletal Science and Sports Medicine Research Centre, Manchester Metropolitan
6 University, Manchester, United Kingdom

7

8 Corresponding author: Jaylene S. Pratt

9 Department of Biomedical Physiology and Kinesiology, SFU, 8888 University Dr, Burnaby, BC

10 V5A 1S6

11 Phone: (778) 782-8445

12 Fax: (778) 782-3040

13 jaylene_pratt@sfu.ca

14 **ABSTRACT**

15 **Purpose:** Producing a steady cadence and power while cycling results in fairly consistent average
16 pedal forces for every revolution, though small fluctuations about an average force do occur. This
17 force can be generated by several combinations of muscles, each with slight fluctuations in
18 excitation for every pedal cycle. Fluctuations such as these are commonly thought of as random
19 variation about average values. However, research into fluctuations of stride length and stride time
20 during walking shows information can be contained in the order of fluctuations. This order, or
21 structure, is thought to reveal underlying motor control strategies. Previously, we found persistent
22 structure in the fluctuations of EMG signals during cycling using Entropic Half-Life (EnHL)
23 analysis. These EMG signals contained fluctuations across multiple timescales, such as those
24 within a burst of excitation, between the burst and quiescent period of a cycle, and across multiple
25 cycles. It was not clear which sources of variation contributed to the persistent structure in the
26 EMG. **Methods:** In this study, we manipulated variation at different timescales in EMG intensity
27 signals to identify the sources of structure observed during cycling. Nine participants cycled at a
28 constant power and cadence for 30 minutes while EMG was collected from six muscles of the leg.
29 **Results:** We found persistent structure across multiple pedal cycles of average EMG intensities,
30 as well as average pedal forces and durations. Additionally, we found the EnHL did not quantify
31 fluctuations within a burst of EMG intensity; instead, it detected unstructured variation between
32 the burst and quiescent period within a cycle. **Conclusions:** The persistent structure in average
33 EMG intensities suggests that fluctuations in muscle excitation are regulated from cycle to cycle.
34
35 **Keywords:** muscle, variability, motor control, sample entropy, entropic half-life.

36 INTRODUCTION

37 Variability is ubiquitous in human gait and small fluctuations within gait signals reveal underlying
38 motor control processes at work. Even when performing a constrained task, such as walking on a
39 treadmill at constant belt speed, or walking to the beat of a metronome, a person's stride length,
40 time, and speed fluctuate about average values (1,2). Historically these fluctuations were attributed
41 to random noise in the motor system, but it is now known they are ordered throughout time and
42 hence contain information considered to reveal aspects of the underlying system control (3,4). This
43 temporal organization, or structure, can be generated by simple mechanical mechanisms or by
44 neural command signals (3,5). To investigate the influence of control signals on the structure of
45 gait parameters, we can examine fluctuations within the EMG signals of muscles that produce
46 forces required for gait (6). Multiple control signals throughout the neuromuscular system possess
47 structure; from single motor unit action potentials to multi-muscle coordination patterns, derived
48 from information contained in EMG signals (7,8). Here we will explore structure in EMG intensity
49 signals. While fluctuations in raw EMG signals reflect the time of individual action potentials,
50 fluctuations in EMG intensities reflect the physiological time of a muscle twitch (9).

51

52 To measure structure, previous studies have relied on Sample Entropy (SEn) analysis (10). By
53 matching small motifs of consecutive data points, SEn quantifies the regularity of a signal (11).
54 However, SEn cannot fully account for fluctuations that persist across multiple timescales (12).
55 The Entropic Half-Life (EnHL) was presented by Zandiyeh and colleagues (12) as a metric to
56 account for fluctuations that persist across multiple timescales with physiologically interpretable
57 units. The EnHL quantifies the timescale at which signal structure breaks down. This involves
58 reshaping the original signal such that consecutive data points become further apart, causing any

59 structure present in the original signal to decay towards a random order. The regularity of the
60 reshaped signals is then quantified with SEn and the EnHL marks the transition from, order seen
61 in the original signal, to random order. The EnHL of neuromuscular coordination patterns derived
62 from EMG was used to demonstrate that there was persistent structure contained within EMG (13).
63 Persistent structure has also been found in raw EMG signals and in EMG intensities using EnHL
64 analysis (6,8,14).

65

66 Control signals collected during gait are cyclic and can be discrete or continuous. Cyclic-discrete
67 signals have one datapoint per cycle that summarizes the whole cycle, such as the average EMG
68 intensity per cycle, or the cycle duration. Cyclic-continuous signals have multiple datapoints that
69 vary through time in each gait cycle. In EMG intensity signals, each cycle contains a burst of
70 intensity and a period of quiescence. This repetitive pattern is removed in cyclic-discrete EMG
71 signals because the cycles are summarized with one datapoint per cycle. Thus, the repetitive
72 bursting pattern will not influence the SEn or EnHL of cyclic-discrete EMG signals. Any structure
73 in these signals can then be attributed to ordered variation at timescales longer than one cycle. In
74 cyclic-continuous EMG intensity signals, fluctuations between data points within a cycle are
75 preserved. In addition to variation at timescales longer than one cycle, cyclic-continuous EMG
76 intensity signals contain the variation between each burst of intensity and period of quiescence
77 within the cycle, as well as variation within each burst of EMG intensity. Variation within a burst
78 of EMG intensity is of particular interest because it may represent fine-tuned adjustments to
79 muscular control within each cycle. If variations within a burst of EMG intensity were shown to
80 influence the structure of cyclic-continuous EMG signals, they could reveal aspects about
81 underlying motor control from moment to moment. For example, differences in the frequency of

82 control system interventions to correct balance were revealed through EnHL analysis on centre of
83 pressure signals during postural challenges (15).

84

85 The repetitive variation of a burst of intensity and a period of quiescence within each cycle is
86 thought to dominate the calculation of SEn and EnHL for cyclic-continuous EMG intensity signals
87 (6,8). This cyclic pattern creates structure in the signal that would lead to very low values of SEn
88 if left unfiltered due to the nature of the SEn calculation (16). Thus, any structure contained in
89 variations between data points that are higher or lower frequency than the cycle frequency at which
90 this cyclic pattern occurs will be masked. Previous researchers have damped the influence of the
91 cycle frequency by filtering the EMG signals (6,13). However, EMG burst durations continue to
92 show influence over the EnHL (6,8). It was suggested that the EnHL of cyclic-continuous EMG
93 signals additionally reflects information about fluctuations occurring *within* each burst, as the
94 EnHL of EMG intensity is shorter than the duration of a burst of EMG intensity (6,8). In this study,
95 we will determine the extent to which EnHL can quantify variations within a burst of intensity in
96 cyclic-continuous EMG intensity signals. Although the sensitivity of the SEn measurement to
97 changes in input parameters was recently investigated for discrete and continuous signals (motif
98 length m and error tolerance r ; (16)), it is not known how variation present at different timescales
99 in discrete and continuous cyclic signals affects the structure measured by SEn and EnHL.

100

101 Here we use a pedalling task to determine the influence of variation at different timescales on the
102 structure of discrete and continuous cyclic EMG intensity signals. These timescales include:
103 variation within a burst of EMG intensity, variation between the burst and quiescent period within
104 a cycle, and variation present at timescales longer than one cycle. To investigate variation within

105 a burst of EMG intensity, we compare the EnHL of cyclic-continuous EMG intensity to the EnHL
106 of several bursting square wave signals that are constructed based on the EMG intensity signals
107 but lack intra-burst fluctuations. If these are not different, EnHL is not able to quantify variation
108 within a burst of EMG intensity in cyclic-continuous EMG signals. To investigate variation
109 between the burst and quiescent periods within a cycle, the square waves will be constructed with
110 a progressive increase in variation related to the cycle timing and intensities. We expect to see a
111 progressively shorter EnHL as more variability is added to the generated signals. To investigate
112 variation at timescales longer than one cycle, we use both continuous and discrete cyclic EMG
113 signals. We randomize the cycle order of one set of square waves to remove the influence of
114 ordered variation at timescales longer than one cycle. We then compare the EnHL of this square
115 wave to the EnHL of a square wave with preserved cycle order. If these are not different, then the
116 EnHL is not able to quantify fluctuations at timescales longer than one cycle in cyclic-continuous
117 EMG intensity signals. To directly examine the variation at timescales longer than one cycle, we
118 calculate the EnHL of the average EMG intensity per cycle. Although the EnHL of cyclic-
119 continuous EMG-derived signals was first explored by Enders and co-workers (13), ours is the
120 first study to investigate EnHL of cyclic-discrete EMG signals and thus the first to examine the
121 average variation in EMG across whole cycles. Conducting the EnHL analysis on average EMG
122 intensity per cycle allows investigation of the influence of control signals on the persistence of
123 structure in whole gait cycles. As additional influence may come from translation of those signals
124 into mechanical output through passive properties of the limb, we also determine the EnHL of
125 average pedal forces and cycle durations.

126

127 **METHODS**

128 **Data Collection**

129 We collected EMG and kinetic data from nine male participants (age 30 ± 6 years, height 176 ± 6
130 cm, mass 73 ± 6 kg; mean \pm SD). Each participant gave informed consent and ethical approval
131 was granted by the Institutional Ethics Review Boards at Simon Fraser University. After shaving
132 the skin and cleaning with alcohol, bipolar Ag/AgCl electrodes (10mm diameter, 21mm
133 interelectrode spacing) were placed on the right leg over the mid bellies of the vastus medialis
134 (VM), vastus lateralis (VL), rectus femoris (RF), medial gastrocnemius (MG), lateral
135 gastrocnemius (LG), and soleus (SOL). EMG signals were amplified (gain 1000), band-pass
136 filtered (bandwidth 10–500 Hz; Biovision, Wehrheim, Germany), and sampled at 2000 Hz (16-bit
137 analog-to-digital converter: USB-6210; National Instruments, Austin, TX). Right effective pedal
138 forces (tangential to the crank) were collected from instrumented pedals (Powerforce; Radlabor,
139 Freiburg, Germany) and recorded at 2000 Hz. A pedal switch was recorded at 2000 Hz to
140 determine cycle times.

141

142 After adjusting the bike seat and handlebars to a comfortable position, participants self-selected a
143 cycling cadence and resistance for the experiment through their warm up period. A metronome
144 was played at various cadences and participants were asked to determine a cycling pace and load
145 that would produce a good workout, that they could maintain for 30 minutes. During the data
146 collection phase, the participants cycled at their self-selected cadence to the metronome for 31
147 minutes and were notified of the time every five minutes and at one-minute remaining.

148

149 **EMG intensity and pedal force processing**

150 Noise from electrical line and motion-capture (collected but not reported in this study) was
151 removed from the EMG signals by interpolating the raw frequency-transformed signals across the
152 critical frequencies of 60 Hz, 180 Hz, and multiples of 100 Hz. EMG amplitudes were interpolated
153 from 2 Hz below to 2 Hz above the critical frequencies, which reduced the noise but did not
154 systematically alter the EMG intensity. EMG signals were resolved into EMG intensities using a
155 bank of 11 non-linearly scaled wavelets, where the EMG intensity is a close approximation to the
156 power in the EMG (9). The time resolution of the wavelets reflect the physiological time of a
157 muscle twitch, thus the timescale of the fluctuations in the EMG intensities reflect these motor
158 events (9). The total EMG intensity was calculated as the sum of the intensities from wavelets 1-
159 10 (covering a frequency band of 11 to 432 Hz), and down-sampled to 1000 Hz. We analyzed data
160 from nine participants for the VM, VL, and SOL, and from eight participants for the RF, LG, and
161 MG (one participant for the LG and MG and one participant for the RF were excluded for poor
162 electrode contact). Right effective pedal forces were filtered to reduce line noise and motion
163 capture interference (4th order low-pass Butterworth, cut-off frequency 200 Hz).

164

165 **Cyclic-discrete signals**

166 Cycle durations were calculated from the pedal switch. Pedal forces and EMG intensities were
167 split into pedal cycles, based on the pedal switch, from which an average value was obtained for
168 each cycle. The burst duration for each muscle was the time for which EMG intensity exceeded a
169 threshold that was 5% of the difference between the minimum and maximum intensity of each
170 cycle (17). Quiescent durations were the difference between the cycle durations and burst
171 durations.

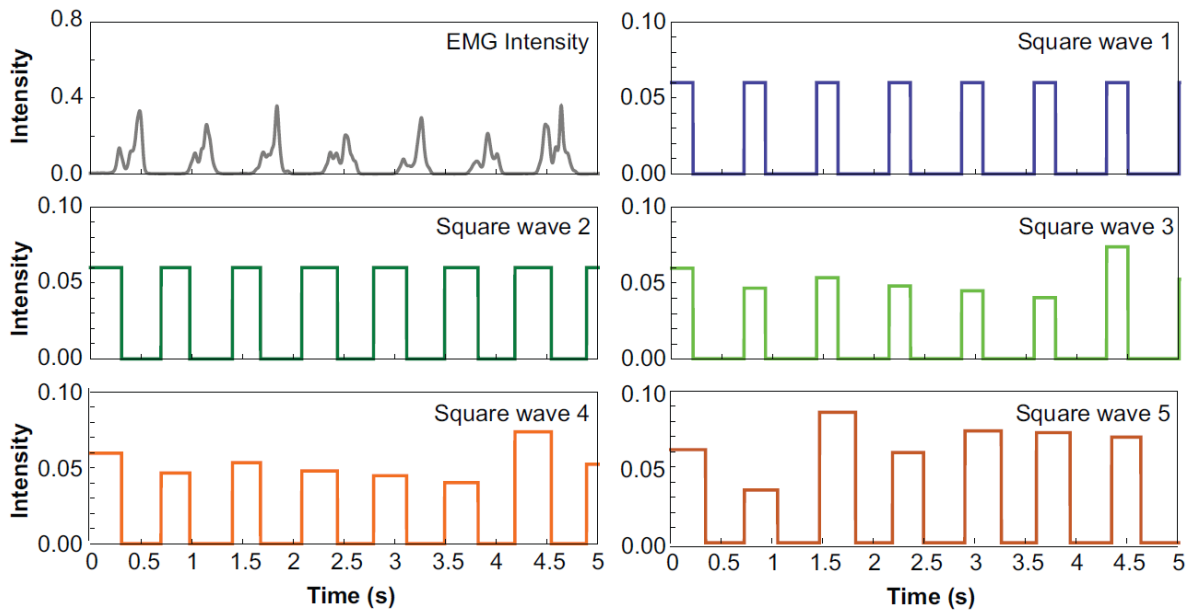
172

173 **Cyclic-continuous EMG intensities**

174 Preliminary work found the EnHL did not differ between 5-minute epochs of the 30-minute cycle.
175 To reduce the computational time of the EnHL analysis, 30 seconds of continuous EMG intensity
176 were analyzed from the beginning of the trial, beginning after one minute of cycling. Four square
177 wave signals were constructed from the burst durations, quiescent durations, and average EMG
178 intensities creating signals ~30 seconds long. For square waves with consistent characteristics, the
179 burst durations, quiescent durations, and burst intensities for each cycle were averaged for each
180 30-second period. All square waves were given a value of 0 for the quiescent period.

181

182 The square waves and EMG intensity for one subject and muscle are illustrated in Figure 1. Square
183 wave 1 had constant burst duration, quiescent duration, and burst intensity for each cycle. Square
184 wave 2 had constant burst intensity but variable burst and quiescent durations for each cycle.
185 Square wave 3 had constant burst and quiescent durations but variable burst intensity for each
186 cycle. Square wave 4 had variable burst intensity as well as variable burst and quiescent durations
187 for each cycle. This resulted in a set of square waves that had a progressive increase in variation
188 of the burst and quiescent characteristics within a cycle but that all lacked variation within a burst
189 of EMG intensity. We created square wave 5 to remove any order in the variation at timescales
190 longer than one cycle. Values from each cycle of square wave 4 were used to construct square
191 wave 5, but we randomized the order of the cycles. This ensured any information related to the
192 order of whole cycles in the original signal would be removed. Consistent with previous work
193 (6,13) the EMG intensities and the square wave signals were filtered to dampen the influence of
194 the cycle frequency on the EnHL (3rd order high-pass Butterworth, cut-off frequency 16 Hz).



195

196 **Figure 1: EMG intensity and constructed square wave signals:** Signals are shown for one
 197 participant for the VM muscle. Square wave 1 has constant burst and quiescent durations and
 198 constant intensity. Square wave 2 has variable burst and quiescent durations but constant burst
 199 intensity. Square wave 3 has variable burst intensity but constant burst and quiescent durations.
 200 Square wave 4 has variable burst and quiescent durations and variable burst intensity. Square wave
 201 5 was constructed by randomizing the cycle order (one burst and one quiescent period) of square
 202 wave 4. 5 seconds of the total 30 second signal are displayed.

203

204 **Sample entropy and reshaping**

205 The entropy analysis was conducted on both the discrete signals (cycle durations, average pedal
 206 forces per cycle, and average EMG intensities per cycle) and the continuous signals (EMG
 207 intensities and square wave signals). All signals were standardized by subtracting the mean and
 208 dividing by the standard deviation. Each signal was then reshaped for scales from 1 cycle (or 1
 209 ms) up to 1000 cycles (or 1000 ms; discrete and continuous signals, respectively) using the process

210 described by Zandiyeh and Von-Tscharner (12). The SEN was calculated for each reshaped signal
211 using open-source software (18) with a motif length of $m=1$ and an error tolerance of $r=0.2$. We
212 tested values of m from 1 to 5 and r from 0.1 to 0.5. Values were chosen to minimize the standard
213 error of the SEN estimate, maximize the number of initial and subsequent template matches, and
214 to produce sigmoidal curves of SEN against reshaping scale. The SEN for each reshaped signal was
215 then normalized according to Equation 1 (19), where $SEN_{reshaped}$ is the SEN of each reshaped signal,
216 $SEN_{original}$ is the SEN of the original signal (reshape scale of 1), and SEN_{random} is the SEN of a
217 completely randomized signal (equivalent to the SEN of the original signal when $m=0$; (11)). This
218 allowed the EnHL to be determined in signals with low initial SEN, which were observed for the
219 discrete signals. This normalization procedure differed from our previous work for the cyclic-
220 continuous EMG intensities, however preliminary tests revealed the difference in EnHL values
221 from the two calculations to be small (5.7 % or 2.0 ms on average).

222

$$223 \quad SEN_{normalized} = \frac{SEN_{reshaped} - SEN_{original}}{SEN_{random} - SEN_{original}} \quad [1]$$

224

225 **Entropic Half-Life (EnHL)**

226 The EnHL was calculated individually for each participant and muscle. To calculate the EnHL,
227 normalized SEN was plotted against reshape-scale time, creating a sigmoidal curve. The EnHL was
228 interpolated as the reshape-scale time when the normalized SEN equals 0.5 (12). For the cyclic-
229 continuous EMG intensities and square waves, we analyzed all nine participants for the VM, VL,
230 and SOL, and all eight participants with good electrode contact for the LG, MG, and RF. For the
231 cyclic-discrete effective pedal forces and pedal cycle durations, we analyzed all nine participants.
232 For the cyclic-discrete average EMG intensities, one participant each from the VM, VL, RF, and

233 SOL had much lower normalized SEn than all other participants. This produced EnHL values for
234 these participants that were 15-57 times greater than the interquartile range of the EnHL from all
235 muscles. The EnHL calculated for these participants became strong outliers and they were
236 excluded from further analysis. Therefore, we analyzed eight participants for the cyclic-discrete
237 average EMG intensities of all muscles except for RF, where we analyzed seven participants.

238

239 **Surrogate Analysis**

240 To verify structure revealed through the SEn and EnHL analyses, we used surrogate analysis of
241 the cyclic-discrete and cyclic-continuous signals. The original cyclic-discrete signals were
242 randomized in time to create surrogate signals with identical distributions but random order. The
243 surrogate signals were then reshaped and SEn calculated for each reshaping scale using the same
244 procedure as the original cyclic-discrete signals. For the surrogate cyclic-discrete signals, the
245 normalized SEn was close to the maximum of one across all reshaping scales (where one represents
246 a randomized signal). Order in the surrogate cyclic-discrete signals was thus random before any
247 reshaping occurred, preventing calculation of the EnHL. To verify structure contained in the
248 original cyclic-discrete signals, we therefore compared the SEn of the original signals before
249 reshaping to the SEn of the surrogates before reshaping.

250

251 For the cyclic-continuous EMG intensities, we created phase-randomized surrogate signals. These
252 retain identical distributions and power spectra to the original signals but do not possess structure
253 related to the phase of the signal (6,13). We applied a Fourier transform to the raw EMG signals
254 and randomized the phase, then performed an inverse Fourier transform. We then calculated the

255 EMG intensities of these phase-randomized signals, and calculated the EnHL using the same
256 procedure as the original cyclic-continuous EMG intensities.

257

258 All above analyses were conducted in Wolfram Mathematica Version 12.1.1 (20) with exception
259 of the SEn calculation which was conducted using a C executable file called through Mathematica.

260

261 **Statistics**

262 To test the difference in EnHL between the EMG intensities and square waves 1-5 we used a linear
263 mixed effects model, conducted with the function *lmer* in the package *lme4* in *R* (21). Signal type
264 (EMG intensity or the five square waves) was modelled as a fixed effect, while subject and muscle
265 were modelled as crossed (not-nested) random effects, accounting for a random intercept of each.
266 The data were positively skewed and a Box-Cox transformation was applied to improve normality.
267 This did not change the results of the analysis, thus we report the results before transformation.
268 Post-hoc analyses were conducted with Tukey's method using the function *glht* in the package
269 *multcomp* (22) and a Holm correction for multiple comparisons was applied (23). Values are
270 reported as mean and standard error across all participants.

271

272 **RESULTS**

273 All participants maintained their self-selected cadences and powers for the duration of the task,
274 which were ~86 rpm and ~130 W respectively. As cadence varied slightly between participants,
275 the total number of cycles (and thus length of the data) analyzed for the discrete signals was
276 between 2077 and 2828.

277

278 **EnHL of cyclic continuous signals**

279 The EnHL of the EMG intensities were higher than their phase-randomized surrogates for each
 280 participant and muscle. The mean EnHL of the phase-randomized surrogate EMG intensities was
 281 6.7 ± 0.02 ms. The mean EnHL of the EMG intensities ranged from 25.1 ± 1.0 ms (RF) to $50.2 \pm$
 282 1.1 ms (SOL) (Figure 2). The sigmoidal curves used to calculate EnHL were visually similar
 283 between the EMG intensities and the generated square waves. p-values from the post-hoc analysis
 284 are reported in Table 1. We were unable to detect a difference between the EnHL of the EMG
 285 intensities and square waves 2-5 (Table 1). Square wave 1 (with constant burst and quiescent
 286 periods) had longer EnHL than the EMG intensities (Table 1), ranging from 36.9 ± 1.9 (MG) to
 287 64.0 ± 4.0 ms (LG) (Figure 2).

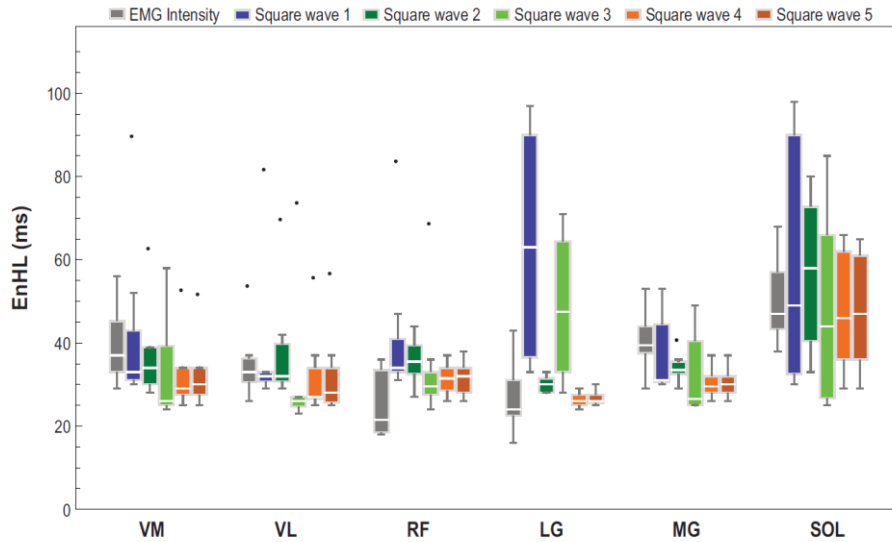
288

Table 1: Comparing EnHL of cyclic-continuous signals: Holm-corrected p-values

	EMG intensity	Square wave 1	Square wave 2	Square wave 3	Square wave 4	Square wave 5
EMG intensity	–	–	–	–	–	–
Square wave 1	0.001*	–	–	–	–	–
Square wave 2	1	0.022*	–	–	–	–
Square wave 3	1	0.006*	1	–	–	–
Square wave 4	1	4.66×10^{-6} *	0.421	0.800	–	–
Square wave 5	1	5.32×10^{-6} *	0.421	0.800	1	–

p-values from the post-hoc test of the linear mixed effects analysis are shown. We compared the EnHL of EMG intensities to the EnHL of five square wave signals lacking intra-burst fluctuations. * indicates low p-value. Square wave 1 had longer EnHL than all other signals.

289



290

291 **Figure 2: EnHL of the cyclic-continuous EMG intensities and the square wave signals.** The
 292 boxes represent the median and interquartile range of EnHL's for each muscle. The whiskers show
 293 the minimum and maximum EnHL, with any outliers displayed as points above the maximum
 294 values.

295 As the variation of the square wave signal increased, the EnHL tended to decrease (Figure 2). The
 296 bursting structure thus decayed at a faster rate. For five of six muscles, the mean EnHL decreased
 297 if variable time was included (square wave 2). For five muscles, the mean EnHL further decreased
 298 if instead, variable intensity was included (square wave 3). And for five muscles, the mean EnHL
 299 yet further decreased if both variable intensity and time were included (square wave 4).
 300 Randomizing the order of the bursts (in square wave 5) had no effect on the EnHL as most
 301 participants showed identical EnHL between square waves 4 and 5 (Figure 2).

302

303 **EnHL of cyclic discrete signals**

304 The SEn of the original cyclic-discrete signals before reshaping was lower than the randomized
 305 surrogates for all individuals, muscles, and discrete signal types. The mean SEn of the original

306 cycle durations, pedal forces, and EMG intensities were 1.64 ± 0.04 , 1.67 ± 0.03 , and 1.75 ± 0.01 ,
 307 respectively; while the mean SEn of the randomized cycle durations, pedal forces, and EMG
 308 intensities were 2.13 ± 0.01 , 2.01 ± 0.03 , and 1.92 ± 0.01 , respectively. EnHL was defined for the
 309 original cycle durations, pedal forces, and EMG intensities (Table 2). Little to no differences were
 310 observed in the EnHL between these signals. The range of EnHL values between subjects was also
 311 small: the EnHL of the cycle durations ranged from 2-6 cycles while the pedal forces ranged from
 312 2.5-7 cycles. After outlier removal, the EnHL of the EMG intensities occupied a similar range, of
 313 2-8 cycles, with one participant showing an EnHL of 14 cycles for RF. Full results including
 314 outliers are reported in the Supplementary Material.

315

Table 2: Entropic Half-Life of the cyclic-discrete signals

	Pedal Cycle Durations	Effective Pedal Forces	Average EMG Intensities					
			VM	VL	RF	LG	MG	SOL
EnHL (number of cycles)	3.00 ± 0.16	3.61 ± 0.15	4.25 ± 0.23	3.94 ± 0.26	5.60 ± 0.6	2.25 ± 0.06	2.44 ± 0.08	3.19 ± 0.16

Values are mean \pm standard error.

316

317 DISCUSSION

318 We explored the effect of fluctuations at different timescales on the persistence of structure in
 319 EMG. The EnHL was unable to detect variation within a burst of EMG intensity or variation across
 320 multiple cycles in cyclic-continuous EMG intensities. The EnHL instead quantified unordered
 321 variation between burst and quiescent durations of a cycle. Additionally, we found persistent
 322 structure at timescales longer than one cycle in cyclic-discrete average EMG intensities, pedal
 323 forces, and cycle durations. Thus, information was shared across consecutive pedal cycles.

324

325

326 **Cyclic-continuous EMG intensities: variation within a burst of EMG intensity**

327 The cyclic nature of the continuous signals strongly dominated the persistence of structure, despite
328 filtering to dampen the cycle frequency. We created a set of square waves with varied burst
329 duration, quiescent duration, and burst intensity to mimic EMG intensity signals with intra-burst
330 fluctuations removed (Figure 1). All square waves with variable intensity, time, or both displayed
331 similar EnHL to the EnHL from the EMG intensity signals (square waves 2-5) despite lacking
332 fluctuations within each burst of intensity. This indicates EnHL analysis does not resolve
333 fluctuations within a burst of EMG intensity in cyclic-continuous EMG signals.

334

335 Why might it be that the EnHL cannot resolve fluctuations within a burst of EMG intensity? A
336 signal that repetitively bursts on and off will contain many more frequencies than the cycle
337 frequency. After filtering to dampen the cycle frequency, structure will remain in the time series,
338 evident as periods of quiescence and periods of excitation. The difference between a point in the
339 quiescent period and a point in the excitation period will be large, while the difference between
340 two points within a quiescent period (or two points within an excitation period) will be much
341 smaller. Points within quiescent or excitation periods will thus be more likely to match throughout
342 the signal, which will contribute to a decreased SEn (i.e. indicating greater regularity in the signal).
343 Points between quiescent and excitation periods will instead contribute to increase the SEn. As the
344 signal is progressively reshaped, more transitions will develop between the quiescent and
345 excitation periods. Thus, the SEn of the signal will progressively increase. The transition of this
346 progression from low to high SEn is measured by the EnHL, explaining why EnHL reflects the
347 bursting parameters of EMG in previous work (6,8,14). It is important to remember that the EnHL
348 does not tell us the moment structure disappears but rather the half-life of the time it takes structure

349 to decay throughout the reshaping process. At the highest SEn, transitions between the quiescent
350 and excitation periods will appear most random. If quiescent and excitation periods are longer, the
351 signal will require more reshaping scales to decay towards random order. The physiological
352 interpretation of the value we obtain for the EnHL in cyclic-continuous EMG signals is that it is
353 related to the duration of the burst and rest periods.

354

355 **Cyclic-continuous EMG intensities: variation between the burst and quiescent period within**
356 **a cycle and variation at timescales longer than one cycle**

357 The EnHL of square wave 1 was significantly different than the EnHL of the EMG intensities
358 (Table 2). Square wave 1 was constructed with a constant burst duration and quiescent duration.
359 This square wave still contained some variation within a cycle due to the repetitive pattern of
360 excitation and quiescence. However, this square wave lacked variation across multiple cycles, as
361 the pattern in each cycle was identical. Variation in the burst and quiescent period across multiple
362 cycles is reflected by the EnHL because square wave 1 had different EnHL from all of the other
363 square waves and from the EMG intensities. Variations in the burst and quiescent durations can
364 also be measured as variation in the cycle durations and duty cycles. Previous work found the
365 EnHL reflects differences in the average duty cycle of EMG signals collected during different
366 mechanical demands (6). Here we find the EnHL reflects the variation in duty cycle and cycle
367 duration over time across multiple cycles.

368

369 Although the EnHL of cyclic-continuous EMG intensity reflects variation in the burst and
370 quiescent period of a signal, it does not reflect the order of these variations. When we randomized
371 the burst order of the variable intensity and time square waves (square wave 5), the EnHL did not

372 change. This could mean one of two things: one, the EnHL of cyclic-continuous EMG intensity
373 does not reflect variations at timescales longer than one cycle; or two, there was no structure in the
374 original order of these variations. The second of these propositions seems unlikely, as we found
375 structure in the cyclic-discrete EMG signals of average intensity. All variation in the cyclic-
376 discrete average EMG intensities is present at timescales longer than one cycle. Structure in the
377 cyclic-continuous EMG intensities at timescales longer than one cycle must have contributed to
378 the structure we found at these timescales in the cyclic-discrete average EMG intensities as these
379 were derived from the continuous signals. Therefore, we suggest that any structure present at
380 longer timescales cannot be quantified by the EnHL of cyclic continuous EMG signals. Although
381 the EnHL was developed to account for fluctuations across multiple timescales, if signals are cyclic
382 these timescales may be limited and depend on the discrete or continuous nature of the analyzed
383 signals.

384

385 The interpretation of persistent and non-random structure in the EMG intensities differs in some
386 aspects from our previous work. It was proposed that the EnHL could reflect information contained
387 within a burst of intensity, as the values for EnHL are shorter than the duration of a burst (6,8).
388 This information would come from motor unit firing and recruitment patterns. However, here we
389 show the information reflected by the EnHL comes from the EMG burst parameters, rather than
390 the motor unit firing and recruitment parameters. It was additionally thought that the EnHL of
391 cyclic-continuous EMG intensities could reflect the persistence of one pedal cycle's influence on
392 subsequent cycles, due to a conserved order of datapoints across multiple cycles (8). We now show
393 the EnHL is unable to evaluate this persistence. We recommend using the EnHL on cyclic-discrete
394 signals if information related to the organization of multiple cycles is required. It was additionally

395 proposed that the EnHL indicates the number of solutions used by the motor control system to
396 perform a task (14). Our results support this interpretation as the EnHL tended to decrease with
397 greater variation included in the square waves. In future work, it would be interesting to discover
398 if these solutions are structured throughout time. This could be analyzed using cyclic-discrete
399 signals.

400

401 **Cyclic-discrete signals: variation at timescales longer than one cycle**

402 The EnHL analysis revealed non-random persistent structure in the average EMG intensities,
403 average effective pedal forces, and cycle durations. As these discrete signals lack variation within
404 a cycle, the structure observed here resulted from ordered variation across multiple cycles. Because
405 the EnHL reveals the influence of past data points on future data points (12), we have shown that
406 a memory of the previous cycle persists in the generation of subsequent cycles for our discrete
407 signals.

408

409 Fluctuations in average EMG intensity reflect adjustments to muscle excitation from cycle to
410 cycle. The EnHL revealed that this cycle-to-cycle influence (or predictability) decays by half
411 within 2.25 to 5.60 cycles (for the LG and RF respectively). The influence of previous cycles on
412 the current state of the EMG may stem from feedback collected in each cycle that is subsequently
413 used to plan future cycles. If this occurred recursively, the influence of a cycle in the past would
414 persist for multiple cycles into the future. For example, EMG intensity may show a tendency to
415 decrease after a cycle with higher average EMG intensity to maintain the imposed power
416 constraint. Although the EnHL cannot evaluate whether a cycle will tend to increase or decrease
417 following a higher than average value, techniques such as detrended fluctuation analysis (24) could

418 be applied in future work. This is the first study to observe a cycle-to-cycle influence in EMG
419 signals. Previous work (6,8,13,14) investigated signals derived from cyclic-continuous EMG,
420 which were unable to quantify structure at timescales longer than one cycle in this study.

421

422 Structure in the fluctuations of EMG may influence motor output during cycling. Here we find the
423 average pedal forces and cycle durations were also structured and decayed at similar rates to the
424 average EMG intensities. This indicates information was shared between consecutive cycles for
425 the pedal forces and durations. Characteristics of the structure in these signals could be influenced
426 by passive mechanics of the lower limb. Indeed, relationships between consecutive stride times
427 have been explained by a passive dynamic walking model with minimal neural feedback (5). A
428 simple mechanical model may also be able to explain the information sharing we observed
429 between pedal durations. However, characteristics of the structure in the forces and durations of
430 consecutive cycles could also be influenced by active control signals through fluctuations in the
431 EMG. If so, the adjustment of excitation in each cycle may fine-tune the forces required to
432 complete each pedal cycle within a timing goal. More research is needed to determine the extent
433 to which fluctuations in the muscle excitation are reflected in the movements of the limb. For
434 example, analysis approaches such as mutual information can reveal if information in one variable
435 is contained within another variable, and this has been analyzed between neural spike timing and
436 wing torque signals in hawkmoths (25). Putney and co-workers (25) showed that spike timing had
437 a larger influence on wing torque than spike count. In the future, such analysis approaches might
438 be used to determine the difference in influence of EMG signals from several muscles on the
439 structure of pedal forces.

440

441 Structure decayed with a similar rate across all of the cyclic-discrete variables, on average with an
442 EnHL of 3.5 cycles. A similar decay in signal structure (3.3 strides) was reported for stride speed
443 during treadmill walking in a study by Raffalt and Yentes (26). Our results for the EnHL are
444 consistent with those for stride speed but are shorter than the EnHL for stride time (12.4 strides)
445 reported by Raffalt and Yentes (26). Shorter EnHL in our study may be due to differences in task
446 constraints. In our study, cycle duration was constrained with a metronome, whereas in the study
447 by Raffalt and Yentes (26), stride speed was constrained by walking on a treadmill. Constraining
448 the task may cause structure in the signal with the constrained parameter to decay faster, which
449 would lower the EnHL. In our study, if the motor control system allowed extended influence of
450 past on future cycles, participants may have progressively deviated from their power and cadence
451 constraints. It is interesting that even in this constrained task, small fluctuations between cycles
452 exhibited order and not random variation about an average value. By freeing task constraints, such
453 as having participants cycle at their own pace, we may have observed longer EnHL and thus an
454 extended cycle memory in the average EMG intensities and cycle durations. We observed large
455 inter-individual differences in the EnHL of the average EMG intensities before excluding outliers,
456 with the highest EnHL of 168.5 strides (See Supplementary Material). A study by Raffalt and
457 Yentes also showed large inter-individual differences, with the highest EnHL of 48 strides (19).
458 The factors leading to these extreme cases of persistent structure are unknown. Future work may
459 wish to consider investigating the inter-individual differences that lead to long EnHL's, with a
460 larger sample size than used in this study.

461

462

463

464 **Future investigation for intra-burst structure in EMG**

465 We were not able to quantify fluctuations within a burst of EMG intensity with the EnHL of cyclic-
466 continuous EMG signals, as suggested might be possible in other work in EMG (6,8), or as
467 suggested might be possible for fluctuations within each cycle in kinematic data (16). However,
468 the EnHL represents a unique way to quantify the persistence of structure in continuous signals,
469 as signals are progressively resampled until data points lose their associations with one another.
470 EnHL analysis has successfully characterized moment to moment fluctuations in *acyclic*
471 continuous centre of pressure signals collected during standing (27,28). It is possible that EnHL
472 analysis of EMG intensities lacking quiescent periods could detect persistent structure within
473 bursts of intensity, and this warrants further investigation. In EMG, structure within a burst of raw
474 EMG was proposed to result from fluctuations in recruited motor units and fluctuations in motor
475 unit firing statistics (6,8). These reflect continuous modulations to muscle excitation from the
476 nervous system and are of great interest. In this work, we found evidence that muscle excitation is
477 modified from cycle to cycle in a non-random way. Other work has shown that muscle excitation
478 is organized into clusters of similar looking steps in a non-random way (29). This evidence implies
479 that muscle excitation is regulated from step to step or from cycle to cycle, in spite of constant
480 mechanical demands. Further investigation of the fluctuations within each burst of EMG intensity
481 is necessary to discover the limits of this regulation. For example, is muscular excitation also
482 regulated in a non-random way within a cycle? There is evidence to suggest that muscle excitation
483 is indeed regulated within a cycle, at the Piper rhythm frequency. This rhythm results from the
484 combined action of many motor units and can be observed within a burst of EMG intensity as
485 alternating sub-bursts of motor unit excitation and rest at a frequency around 35-60 Hz (30). It was
486 proposed that the brain modifies muscle excitation during a contraction using signals sent out at

487 the Piper rhythm frequency (31). Indeed, changes to the Piper rhythm are observed with altered
488 running speeds and while fatigued (31,32). It may be that muscular excitation is modified in
489 packets of information, the length of one Piper period (17-29 ms). Fluctuations in muscle
490 excitation that at first glance appear random, may in fact be purposeful—perhaps to optimize each
491 moment for task adjustment, efficiency, or fatigue reduction. Further work is needed to test this
492 proposition.

493

494 **Conclusions**

495 We manipulated EMG data collected during cycling to exclude variation at different timescales
496 and explored how variation at different timescales is represented in the structure of EMG.
497 Although cyclic-continuous EMG intensities contained variation within a burst of EMG intensity,
498 this variation did not contribute to the EnHL. Although fluctuations at timescales longer than one
499 cycle existed in the continuous-cyclic EMG intensities, the EnHL of these signals was not
500 influenced by this variation. Instead, the EnHL of cyclic-continuous EMG intensities was largely
501 influenced by unstructured variation between the burst and quiescent periods of a cycle. We
502 additionally found persistent structure in the fluctuations of cyclic-discrete signals of average
503 EMG intensities, average pedal forces, and cycle durations, thus for the first-time revealing
504 information contained in the EMG at timescales longer than one cycle.

505

506 This research was supported by the Natural Sciences and Engineering Research Council of
507 Canada. The authors would like to thank Stephanie Lee for her assistance in data collection.

508

509 There are no professional relationships with companies or manufacturers to disclose for all authors.
510 The results of the present study do not constitute endorsement by the American College of Sports
511 Medicine. The authors declare that the results of the study are presented clearly, honestly, and
512 without fabrication, falsification, or inappropriate data manipulation.

513

514 REFERENCES

- 515 1. Dingwell JB, Cusumano JP. Re-interpreting detrended fluctuation analyses of stride-to-
516 stride variability in human walking. *Gait Posture*. 2010;32(3):348–53.
- 517 2. Terrier P, Turner V, Schutz Y. GPS analysis of human locomotion: Further evidence for
518 long-range correlations in stride-to-stride fluctuations of gait parameters. *Hum Mov Sci*.
519 2005;24(1):97–115.
- 520 3. Hausdorff JM. Gait dynamics, fractals and falls: Finding meaning in the stride-to-stride
521 fluctuations of human walking. *Hum Mov Sci*. 2007;26(4):555–89.
- 522 4. Newell KM, Slifkin AB. The Nature of Movement Variability. In: Piek JP, editor. Motor
523 Behavior and Human Skill: A Multidisciplinary Approach. Human Kinetics Publishers
524 Inc.; 1998. p. 143–60.
- 525 5. Gates DH, Su JL, Dingwell JB. Possible biomechanical origins of the long-range
526 correlations in stride intervals of walking. *Phys A Stat Mech its Appl*. 2007;380:259–70.
- 527 6. Hodson-Tole EF, Wakeling JM. Movement Complexity and Neuromechanical Factors
528 Affect the Entropic Half-Life of Myoelectric Signals. *Front Physiol*. 2017;8:679.
- 529 7. Vaillancourt DE, Larsson L, Newell KM. Time-dependent structure in the discharge rate
530 of human motor units. *Clin Neurophysiol*. 2002;113(8):1325–38.
- 531 8. Wakeling JM, Hodson-Tole EF. How do the mechanical demands of cycling affect the

- 532 information content of the EMG? *Med Sci Sports Exerc.* 2018;50(12):2518–25.
- 533 9. Von Tscharner V. Intensity analysis in time-frequency space of surface myoelectric
534 signals by wavelets of specified resolution. *J Electromyogr Kinesiol.* 2000;10(6):433–45.
- 535 10. Richman JS, Moorman JR. Physiological time-series analysis using approximate and
536 sample entropy. *Am J Physiol - Hear Circ Physiol.* 2000;278:H2039–49.
- 537 11. Richman JS, Lake DE, Moorman JR. Sample Entropy. *Methods Enzymol.* 2004;384:172–
538 84.
- 539 12. Zandiyeh P, Von Tscharner V. Reshape scale method: A novel multi scale entropic
540 analysis approach. *Phys A Stat Mech its Appl.* 2013;392(24):6265–72.
- 541 13. Enders H, Von Tscharner V, Nigg BM. Neuromuscular strategies during cycling at
542 different muscular demands. *Med Sci Sports Exerc.* 2015;47(7):1450–9.
- 543 14. Hodson-Tole EF, Blake OM, Wakeling JM. During cycling what limits maximum
544 mechanical power output at cadences above 120 rpm? *Med Sci Sports Exerc.*
545 2020;52(1):214–24.
- 546 15. Federolf P, Zandiyeh P, von Tscharner V. Time scale dependence of the center of pressure
547 entropy: What characteristics of the neuromuscular postural control system influence
548 stabilographic entropic half-life? *Exp Brain Res.* 2015;233(12):3507–15.
- 549 16. McCamley J, Denton W, Arnold A, Raffalt P, Yentes J. On the Calculation of Sample
550 Entropy Using Continuous and Discrete Human Gait Data. *Entropy.* 2018;20(10):764.
- 551 17. Blake OM, Wakeling JM. Early deactivation of slower muscle fibres at high movement
552 frequencies. *J Exp Biol.* 2014;217(19):3528–34.
- 553 18. Goldberger AL, Amaral LA, Glass L, Hausdorff JM, Ivanov PC, Mark RG, et al.
554 PhysioBank, PhysioToolkit, and PhysioNet: components of a new research resource for

- 555 complex physiologic signals. *Circulation*. 2000;101(23).
- 556 19. Raffalt PC, Yentes JM. Introducing Statistical Persistence Decay: A Quantification of
557 Stride-to-Stride Time Interval Dependency in Human Gait. *Ann Biomed Eng*.
558 2018;46(1):60–70.
- 559 20. Wolfram Research Inc. Mathematica [Internet]. Champaign, Illinois: Wolfram Research,
560 Inc.; 2020. Available from: <https://www.wolfram.com/mathematica>
- 561 21. Bates D, Mächler M, Bolker BM, Walker SC. Fitting linear mixed-effects models using
562 lme4. *J Stat Softw*. 2015;67(1):1–48.
- 563 22. Hothorn T, Bretz F, Westfall P. Simultaneous inference in general parametric models.
564 *Biometrical J*. 2008;50(3):346–63.
- 565 23. Holm S. A simple sequentially rejective multiple test procedure. *Scand J Stat*. 1979;6:65–
566 70.
- 567 24. Peng CK, Havlin S, Stanley HE, Goldberger AL. Quantification of scaling exponents and
568 crossover phenomena in nonstationary heartbeat time series. *Chaos*. 1995;5(1):82–7.
- 569 25. Putney J, Conn R, Sponberg S. Precise timing is ubiquitous, consistent, and coordinated
570 across a comprehensive, spike-resolved flight motor program. *Proc Natl Acad Sci U S A*.
571 2019;116(52):26951–60.
- 572 26. Raffalt PC, Yentes JM. On the application of entropic half-life and statistical persistence
573 decay for quantification of time dependency in human gait. *J Biomech*. 2020;108:109893.
- 574 27. Baltich J, von Tscherner V, Zandiyeh P, Nigg BM. Quantification and reliability of center
575 of pressure movement during balance tasks of varying difficulty. *Gait Posture*.
576 2014;40(2):327–32.
- 577 28. Ferrari E, Cooper G, Reeves ND, Hodson-Tole EF. Intrinsic foot muscles act to stabilise

578 the foot when greater fluctuations in centre of pressure movement result from increased
579 postural balance challenge. *Gait Posture*. 2020;79:229–33.

580 29. Von Tscharner V, Ullrich M, Mohr M, Comaduran Marquez D, Nigg BM. A wavelet
581 based time frequency analysis of electromyograms to group steps of runners into clusters
582 that contain similar muscle activation patterns. *PLoS One*. 2018;13(4).

583 30. Stirling LM, von Tscharner V, Kugler P, Nigg BM. Piper rhythm in the activation of the
584 gastrocnemius medialis during running. *J Electromyogr Kinesiol*. 2011;21(1):178–83.

585 31. Maurer C, Von Tscharner V, Nigg BM. Speed-dependent variation in the Piper rhythm. *J*
586 *Electromyogr Kinesiol*. 2013;23(3):673–8.

587 32. von Tscharner V, Barandun M, Stirling LM. Fatigue-related decrease in Piper rhythm
588 frequency of the abductor pollicis brevis muscle during isometric contractions. *J*
589 *Electromyogr Kinesiol*. 2011;21(1):190–5.

590

591

Supplementary Table 1: Entropic Half-Life of the cyclic-discrete signals

Participant Number	Number of Analyzed Cycles	Pedal Cycle Durations	Effective Pedal Forces	EnHL (number of cycles)					
				Average EMG Intensities					
				VM	VL	RF	LG	MG	SOL
1	2828	4	4	3	112	168.5	2	3.5	3
2	2526	3	3.5	2.5	2	3	2	2	47
3	2526	4	3	7.5	5.5	2	2	2	4
4	2475	2	2.5	5	3	n/a	3	3	3
5	2077	2	2.5	3.5	2	6.5	2	2	2
6	2628	2	7	6	2.5	8	2	2	6
7	2711	6	3.5	4.5	3.5	3.5	n/a	n/a	3
8	2508	2	3	101.5	5	14	2	2	2.5
9	2478	2	3.5	2	8	2	3	3	2

Participants with 'n/a' are those with poor electrode contact.

The EnHL of the cyclic-discrete signals for all participants is shown above, including the outliers which were removed to calculate the mean and standard error in the main text. The participants with large EnHL for some muscles appeared to show long-term trends in the average EMG intensities over the 30-minute pedaling task. The number of cycles analyzed for each participant was also large. Future investigations into the factors leading to long EnHL's may wish to include the influence of signal duration.